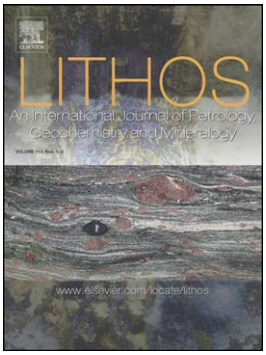

Ion microprobe dating of zircons from active Dayingshan volcano, Tengchong, SE Tibetan Plateau: Time scales and nature of magma chamber storage

Ross T. Tucker, Haibo Zou, Qicheng Fan, Axel K. Schmitt

PII: S0024-4937(13)00134-5
DOI: doi: 10.1016/j.lithos.2013.04.017
Reference: LITHOS 2974

To appear in: *LITHOS*

Received date: 3 November 2012
Accepted date: 18 April 2013

Please cite this article as: Tucker, Ross T., Zou, Haibo, Fan, Qicheng, Schmitt, Axel K., Ion microprobe dating of zircons from active Dayingshan volcano, Tengchong, SE Tibetan Plateau: Time scales and nature of magma chamber storage, *LITHOS* (2013), doi: 10.1016/j.lithos.2013.04.017

Ion microprobe dating of zircons from active Dayingshan volcano, Tengchong, SE Tibetan Plateau: time scales and nature of magma chamber storage

Ross T. Tucker[1], Haibo Zou[*,1], Qicheng Fan[2] and Axel K. Schmitt[3]

1 Department of Geology and Geography, Auburn University, Auburn, AL 36849, USA

2 Institute of Geology, China Earthquake Administration, Beijing 100029, China

3 Department of Earth and Space Sciences, University of California, Los Angeles, CA 90095, USA

****

*Corresponding author:

H. B. Zou

Haibo.zou@auburn.edu

Phone: 334-844-4315

ABSTRACT

The rare occurrences of active volcanoes on the Tibetan Plateau provide a unique opportunity to investigate time scales of magma chamber processes for post-collisional potassic volcanism. This research utilizes high-spatial resolution U-Th disequilibrium dating methods to date zircons from the active Dayingshan volcano, Tengchong, SE Tibetan Plateau, which erupted last during the Holocene. Zircon crystal ages can be used to provide constraints on the magma chamber storage time. Measured zircon interiors yielded an isochron age of 87.5 ± 6.5 ka, while zircon outermost rims yielded an isochron age of 58 ± 13 ka. The calculated zircon crystal storage time for the most recent eruption is 48 ka. At least two separated late Pleistocene zircon crystallization events have occurred where the older age population represents antecrysts remobilized from an earlier magmatic episode, but protracted crystallization cannot be ruled out. Regardless, the similarity in zircon age populations between Dayingshan volcano and Maanshan volcano 13 km apart in the Tengchong volcanic field suggests a synchronous thermal history of the magma reservoir, possibly in an extensive interconnected magma chamber beneath the Tengchong volcanic field.

Key words. U-Th disequilibrium, young zircon, magma residence times, Tengchong, Tibet.

1. Introduction

Volcanism in the Tibetan Plateau has been occurring throughout the Cenozoic concurrent with the development of the Himalaya orogen and uplift of the Tibetan Plateau. The Tengchong volcanic field (TVF; 24°40'-25°30'N, 98°15'-98°45'E) is located in the southeastern portion of the Tibetan Plateau, and has recorded volcanism from ~ 5 Ma to <10 ka (Zhu et al., 1983; Zou et al., 2010). Maanshan, Dayingshan, and Heikongshan are the three most recently active volcanoes in the TVF, each with recorded Holocene (<10 ka) eruptions. The volcanism is derived from a potassic melt, and is post-collisional, as the continental collision that developed the Himalayas initiated much earlier (~65 Ma). There are numerous hot springs in the area, indicating active geothermal fields that show potential for volcanic eruptions.

High-spatial resolution U-Th dating of young zircons using secondary ionization mass spectrometry (SIMS) has been useful for constraining time scales of magma chamber processes (Reid et al., 1997; Vazquez and Reid, 2002; Charlier et al., 2005; Bacon et al., 2007; Zou et al., 2010b). This is because zircons are enriched in U relative to Th and have a large spread in U/Th ratios, allowing for the recording of the pre-eruptive history of a magma up to 350 ka. Crystal storage time can thus be discerned by subtracting the age of the last eruption event from the age of the zircons in the sample rock. In a simple scenario, if zircon crystallization occurred entirely within the erupted magma, crystal and magma residence times are equivalent. Antecrystic zircon, by contrast, can also be derived from earlier solidified portions of the magma chamber. This has been proposed based on comparison of zircon age populations in cogenetic volcanic and plutonic rocks (e.g., Schmitt et al., 2003). In other cases, zircon has been recycled

through remelting of deeply subsided intra-caldera volcanic rocks (e.g., Simakin and Bindeman, 2011). If antecrystic, crystal residence times place an upper bound on magma residence times.

Because the ability to resolve age differences decreases with rock age, the most informative data about residence time scales come from young eruptions (Simon et al., 2008). We thus choose active volcanoes to study time scales of post-collisional volcanism at SE Tibetan Plateau.

Holocene volcanic rocks from the Tengchong volcanic field contain zircon crystals suitable for U-Th disequilibrium studies (Zou et al., 2010a). This research attempts to better constrain magma storage time prior to eruption by analysis of samples from the active Dayingshan volcano, the largest of the three active volcanoes in the Tengchong volcanic field.

==========

Fig. 1A, 1B, 1C, 1D

==========

Dayingshan volcano has been extensively studied, including detailed geochemical, petrological, and geophysical investigations (Zhu et al., 1983; Mu et al., 1987a; Bai et al., 2001; Fan et al., 2001; Chen et al., 2002; Wei et al., 2003; Wang et al., 2006; Zhao et al., 2006; Lei et al., 2009; Zhao and Fan, 2010; Guo et al., 2011; Zou and Fan, 2011; Xu et al., 2012; Zhou et al., 2012). Crystal-scale analysis of crystallization time scales and magma residence are still lacking. It is also not clear if Dayingshan volcano shares a common magma reservoir with other active volcanoes in Tengchong.

The main objectives of this study are to: (1) determine the age(s) of zircon crystallization events from Dayingshan volcanic rocks using high-spatial-resolution zircon U-Th dating methods; (2) constrain the duration of magma chamber storage before an eruption for an intracontinental, potassic magma system; and (3) compare the Dayingshan zircon data with data for Maanshan volcano (Zou et al., 2010a) to evaluate whether or not these two volcanoes share a common magma reservoir. Magmatic timescales and processes inferred from U-Th disequilibrium in the Tengchong lavas can also elucidate these processes in other post-collisional magmatic systems in Tibet where high temporal resolution analysis is precluded by their older ages.

2. Tengchong volcanic field and Dayingshan volcano

The Tengchong volcanic field is located along the southeastern margin of Tibetan plateau in the Yunnan province of China. The field is in close proximity to the border of China and Burma, and sits ~450 km from the Indian plate. The field lies in a structurally complex area due to several faults and suture zones that run through and intersect in the area. The Sagaing dextral fault, Myitkyina suture zone, and Burma gneissic belt lie west of the field, while the Gaoligong metamorphic belt and Red River fault zone lie to the east. This has created a N-S fault zone in which the field is situated. Most of these faults formed as a result of the continental collision between India and Asia. Further to the West is the Burma volcanic arc. Volcanism has also been active since the late Tertiary (Huangpu and Jiang, 2000; Wei et al., 2003), but its initiation significantly post-dates the onset of collision initiated the Indo-Australian and Eurasian plate (~65 Ma). The field is

unique in that it is the only active volcanic zone in the region, as recent geothermal studies suggest that a magmatic reservoir is still present beneath the field (Bai et al., 2001).

There are 68 volcanoes in the Tengchong volcanic field (Huangpu and Jiang, 2000). Older periods of volcanism are evident in the northern and southern parts of the field, while more recent eruptions have migrated to the central part (Wang et al., 2006). Eruptions in the Tengchong area can be divided into four major stages: late Miocene-Pliocene basalt and olivine-basalt volcanic rocks (5.5-4.0 and 3.8-0.9 Ma), Pleistocene andesites and dacites (0.8-0.1 Ma), and late Pleistocene-Holocene basalts and basaltic andesites (0.1 to less than 0.01 Ma) (Mu et al., 1987b; Jiang, 1998; Huangpu and Jiang, 2000; Li et al., 2000).

Older eruptions in the Tengchong volcanic field are composed of dominantly basaltic rocks, whereas more andesitic rock types are associated with the three youngest Holocene volcanoes, Maanshan, Dayingshan, and Heikongshan. Rocks associated with this recent volcanism also contain high abundances of potassium. Wang et al. (2006) reported a 1.5 to 3.65% increase in K_2O content from the Pliocene to Holocene. Volcanic rocks in the area typically contain high abundances of Al_2O_3 and K_2O and low abundances of TiO_2 (Wang et al., 2006). The field's location in a N-S trending fault zone has led to the eastern and western parts of the area being uplifted while the central region has been depressed, creating elevation differences of more than 500 m (Wang et al., 2007). Total crustal thickness in the region is 40-50 km (Zhu et al., 1983).

The Dayingshan volcano experienced 4 episodes of eruptions throughout the Holocene (Huangpu and Jiang, 2000). The first eruption produced andesite lavas; the

second and third eruptions were explosive, producing volcaniclastic rocks. The third eruption also generated a large scoria cone with a caldera. Finally, during the fourth event trachyandesite lavas erupted. There is a hiatus indicated by a 20 cm thick paleosol between episodes 1 and 2. No discernable hiatus exists between episodes 2, 3 and 4. Figure 1D shows the distribution of the depositional units erupted from Dayingshan. Currently, there are on-going earthquake and hydrothermal activities in the area (Shangguan et al., 2005).

The volcanic rocks from Dayingshan volcano have SiO_2 greater than 60%, higher than both Maanshan and Heikongshan volcanoes, representing the most evolved magmas in the volcanic field (Fan et al., 1999). The sample of this study is from the youngest (fourth) Dayingshan eruption (Fig. 2). The mineral constituents of the rock are plagioclase and pyroxene phenocrysts (~10-15%) in a matrix consisting mostly of plagioclase, olivine, augite, and volcanic glass. This sample contains euhedral zircons with long dimensions up to 350 μm.

3. Analytical Methods

3.1. Zircon

Samples were crushed using a rock hammer and are grinded using a brand-new laboratory disc mill. Zircons were separated using magnetic and conventional heavy liquid (methylene iodide) separation. Individual crystals were picked from the heavy mineral separates using a fine-point needle under an optical microscope.

After the separation process, the zircons were prepared and mounted for SIMS by embedding the grains in indium, followed by washing in dilute HCl and methanol, oven-drying (~50°C), and coating with a thin (20-40 nm) gold layer to generate a conducting sample surface. Unpolished zircons with flat crystal surfaces were used for shallow depth profiling which provides enhanced spatial resolution on natural crystal surfaces. Depth profiling has been applied to Th-Pb monazite dating (Grove and Harrison, 1999), U-Pb zircon dating (Reid and Coath, 2000), and U-Th disequilibrium zircon dating (Zou et al., 2010a; Schmitt, 2011; Storm et al., 2011).

Analyses were performed using the CAMECA ims 1270 at the NSF National Ion Microprobe Facility at the University of California, Los Angeles (UCLA). The sample was sputtered with a primary beam of $^{16}O^-$ ions generated in a duoplasmatron ion source in order to obtain rim ages. Zircon sputter rates are ~0.05 μm^3/nA/sec (Schmitt, 2011), and the typical duration rate to sputter one zircon is ~20 minutes.

After measuring the unpolished zircons, the mount was then removed from the sample chamber, polished to a depth of 3 μm and cleaned as before. After re-coating them with new thin Au layer, the interior of the exposed zircon crystals was targeted to obtain interior ages.

Because a relatively flat crystal face is needed in order to accommodate the ion beam, it is important to note that fewer zircons were measured during the unpolished measurements due to a smaller percentage of zircons demonstrating euhedral prism faces oriented flush with the mount surface.

$^{230}Th/^{232}Th$ and $^{238}U/^{232}Th$ analyses with the Cameca ims 1270 achieves an average precision of ~1-2 %. Key secondary ion intensities measured by SIMS U-Th

dating are $^{230}Th^{16}O^{+}$, $^{232}Th^{16}O^{+}$, and $^{238}U^{16}O^{+}$. $^{90}Zr_2{}^{16}O_4{}^{+}$ is also measured as a reference to estimate uranium abundances. The low-intensity $^{230}Th^{16}O^{+}$ peak is corrected for backgrounds measured at mass/charge of 244.03 and 246.3, and are gain corrected to ensure accurate counts and calibration. AS-3 zircons from the Duluth Complex were used as standards to calibrate the relative sensitivities for ^{238}UO, ^{232}ThO and ^{230}ThO (Schmitt, 2009). Radiogenic $^{206}Pb/^{208}Pb$ is measured in the AS-3 zircons rather than Th/U because in old, concordant zircons with known ages, the radiogenic $^{208}Pb/^{206}Pb$ is a unique function of the Th/U atomic ratio (Reid et al., 1997; Zou et al., 2010a); therefore, a Th/U relative sensitivity factor can be calculated. The primary current was generated at ~40-80 nA, and the secondary ions were analyzed at a mass resolving power of ~5000.

3.2. Whole rock

Whole-rock major element compositions were measured by X-ray fluorescence (XRF) and trace element concentrations were measured by ICP-MS at the GeoAnalytical Lab, Washington State University. Sample powders were prepared with an agate mill to avoid potential contamination of Ta and Nb by a tungsten carbide mill.

4. Dayingshan whole-rock sample

The major and trace element concentrations of sample DA09026 from Dayingshan are given in Table 1. The sample is classified as trachyandesite. Of

particular interest is the high Zr concentration of 329 ppm given by ICP-MS analysis. Note that XRF analysis yields 322 ppm Zr, consistent with ICP-MS Zr data. The Dayingshan rock sample is metaluminous, with an alumina saturati*on* index (ASI) molecular ratio ($Al_2O_3/(CaO+K_2O+Na_2O)$) of 0.88 and $Al_2O_3/(K_2O+Na_2O)$ of 1.58. This metaluminous composition, coupled with high Zr concentrations, would likely stabilize zircon unless temperatures exceeded the zircon saturation (see below).

==========

Table 1. Major and trace element concentrations

==========

Multi-element normalized trace element patterns (Fig. 2) for the Dayingshan sample show enrichment in the more incompatible elements, such as Rb and Th, and depletion in elements with high field strengths, such as Nb and Ta. Figure 2 also shows enrichments in LREEs, and depletions in Sr and Eu, consistent with fractional crystallization of plagioclase.

==========

Fig. 2. Multi-element-normalized Diagram

==========

5. Zircon Ages

5.1. Unpolished Zircon Rim Ages

Because the outer rims of Dayingshan zircons (faintly visible in some CL images; grain 10 in Fig. 4) were smaller than the typical beam spot of 25 μm, shallow (< 3 μm) depth profiling analysis of U-Th isotopes (Zou et al., 2010a; Schmitt, 2011) was used. Depth profiling allows for specific targeting of the surface of natural zircon crystal faces. U/Th ages of 17 unpolished zircon grains were measured (Table 2). Grain Day-rim1 was disregarded due to high background readings and Day-rim16 was disregarded due to low U ppm. The U/Th isochron ages of the other 15 zircon rims is 58 ± 13 ka, with a MSWD of 1.8 (Fig. 4). This age data is similar to the calculated age of 53.6 ± 5 ka by Zou et al. (2010) of unpolished zircon rims from Maanshan volcano.

==========

Table 2. U-Th isotope data for unpolished zircon rims

Fig. 3. Unpolished zircon rim U-Th isochron

==========

5.2. Polished Zircon Interior Ages

Zircon interiors were measured by SIMS to attain the ages of the mineral interiors. Selected zircon cathodoluminescence images (for grains 4, 7 and 10) are shown in Figure 4. Twenty-two polished zircon interiors were measured (Table 3), with 21 grains yielding an apparent U/Th isochron age of 87.5 ± 6.5 ka (Fig. 5), with a mean square of weighted deviates (MSWD) of 3.7.

==========

Table 3. U-Th isotope data for polished zircon interiors

Fig. 4. Zircon cathodoluminescence images

Fig. 5. Polished zircon interior U-Th isochron

==========

Grain Day-int16 was disregarded due to an inherently low U ppm. The MSWD value of 3.7 exceeds the threshold for a single age population. Alternatively, we can use zircon-melt two-point model ages to treat the interior data. Using a mixture modeling chart, based on the probability density function, the U/Th model ages of Dayingshan zircon interiors (Fig. 6) can be shown to represent a nearly unimodal population which is slightly skewed to older ages. This data is similar to a calculated age of 91 ± 6 ka for interiors of Maanshan zircons (Zou et al., 2010).

==========

Fig. 6. Zircon interior model age distribution

==========

6. Discussion

6.1. Magma Chamber Storage Time

Constraints on magma storage time in the Tengchong volcanic field are important for several reasons. A better understanding of magma chamber processes could provide valuable insight into the ascent and storage of magma, especially where bulk compositions appear unfavorable for zircon crystallization (Watson and Harrison, 1983). This information could prove valuable to the many people who live in close proximity to the active volcanoes. In large part, industry and tourism attract people into areas within active geothermal fields (Wei et al., 2003).

Calculated interior ages (87.5 ± 6.5 ka) are older than calculated rim ages (58 ± 13 ka), representing two different zircon growth events. For Maanshan volcano, a similarly old population was found to be inconsistent with incorporatation of xenocrysts from basement rocks. However, it may represent zircons that have been remobilized from an earlier magmatic episode (Zou et al., 2010). These zircons were considered antecrysts, in that they grew from predecessor magmas left over in the magma chamber.

Dayingshan zircon ages (58 and 87.5 ka) are also much younger than those expected for country rocks underneath. Regional country rocks include Paleozoic gneisses, Carboniferous sandstones, 76 to 235 Ma Mesozoic granites and 32 to 52 Ma Cenozoic granites. Based on the strong age difference, all Dayingshan zircons measured here are not inherited zircons from country rocks. Therefore, the zircons present must have formed in the magma chamber prior to eruption. We can infer crystal residence times by subtracting the volcanic eruption event that yielded the basaltic andesites from the calculated zircon ages. Using an eruption age of <10 ka (Huangpu and Jiang, 2000; Li and Liu, 2012), a residence time of 48 ka is determined for zircon rims and 77.5 ka for zircon interiors.

Here we interpret the interior ages as antecryst ages and the outermost rim ages as zircon overgrowth ages in a precursor melt. Alternatively, the zircons could have grown continuously from 88 ka and then terminated at 58 ka. Deeper depth profiling would be needed to resolve the possibility of continuous zircon growth (Storm et al., 2011; Shane et al., 2012). In a continuous growth scenario, magmatic residence times would be more protracted than indicated by a relatively short-lived

pulse of rim zircon crystallization. When compared with other small-volume eruptions, the Dayingshan volcano has relatively short magma residence times (Fig. 7). The magma residence times for small volume silicic eruptions range from 25 ka to more than 225 ka (Simon et al., 2008), while the residence time for Dayingshan eruption is about 48 ka with maximum value of 78 ka (in the case of continuous growth).

==========

Fig. 7. Comparison of magma residence times
with other small volume eruptions

==========

The complete absence of xenocrytic zircons from more than 60 zircons from the youngest eruptions in Dayingshan volcano and Maanshan volcano at Tengchong is notable. This contrasts with the presence of a few xenocrytic zircons in older eruptions outside of (to the south of) Maanshan volcano (Li et al., 2012).

6.2. Zircon Saturation

Whether the melt was saturated with respect to zircon is important when trying to interpret possible zircon inheritance from country rocks. Zircon saturation is a function of both magma composition and temperature, and is defined by the equation (Watson and Harrison, 1983):

$$\ln D_{Zr}^{zircon/melt} = (-3.80 - [0.85(M-1)]) + \frac{12900}{T}$$

where $D_{Zr}^{zircon/melt}$ is the concentration ratio of Zr in zircon to Zr in the melt, M represents the melt composition ((Na+K+2Ca)/(Al×Si)), and T is the temperature in Kelvin. This study uses zircon saturation as a means to assess the likelihood for zircon inheritance in the system. According to major element compositions in Dayingshan sample DA09026, M = 1.97. An estimated temperature of 750°C is used based on Ti-in-zircon geothermometry from Maanshan (Zou et al., 2010). Using these two variables, the Zr concentration needed to saturate the melt is 170 ppm. Because whole-rock analysis yielded a Zr concentration of 329 ppm, and only 170 ppm is needed to saturate the melt, we can infer that zircon was stable in the melt. Under these conditions, any zircons derived from country rocks would remain stable in the melt, and form an inherited population. The complete absence of zircon inheritance suggests that late-stage crustal contaminations through assimilation of country rocks is insignificant.

Although we have no direct temperature constraints for the Dayingshan magma, and acknowledge significant uncertainties in the Ti-in-zircon thermometer (~50°C because of uncertainties in pressure and TiO_2 activity), the higher Zr abundances and lower M values for Dayingshan compared to Maanshan conspire to yield higher zircon saturation temperatures for Dayingshan. Dayingshan magma was thus zircon saturated at the time of eruption.

6.3. Th/U Ratios

Dayingshan zircons have higher than average Th/U ratios for igneous zircons. An average Th/U ratio for most igneous zircons is ~0.5, and typically

ranges from 0.2 - 0.9 (Bindeman et al., 2006). Unusually high Th/U ratios are often indicative of a continental crustal component in the melt. Dayingshan cores have an average Th/U ratio of 1.92, and range from 0.71 – 3.95. Dayingshan rims have an average Th/U ratio of 1.58, and range from 0.68 – 3.46. Although the variation in Th/U ratios is high, zircon rims yielded only slightly lower ratios than zircon cores. A rimward decrease in Th/U ratios is indicative of fractionation during zircon growth (Zou et al., 2010). Despite the slight difference in Th/U ratios, the similarity between interior and rim ratios suggests the crystals share a closed-system evolution, implying contamination in the magma system since the zircon core formation is minimal (Zou et al., 2010).

In order to determine if the high Th/U ratios in the Dayingshan zircons are a result of high Th/U ratios in the original melt, the mineral/melt partitioning coefficients ($D_{Th/U}$) for the concentrations of Th and U were determined. $D_{Th/U}$ is the ratio of concentration of U and Th in a crystallizing zircon to concentration of these elements in the melt. $D_{Th/U}$ is calculated by the following equation:

$$D_{Th/U} = \frac{Th_{zircon} / U_{zircon}}{Th_{melt} / U_{melt}}$$

The whole-rock Th and U concentrations are 33.48 ppm and 3.22 ppm, respectively (Table 1). Thus the melt Th/U ratio is 10.4. Using this equation, and a Th/U melt ratio of 10.4, the average $D_{Th/U}$ is 0.18 ± 0.07 for zircon interiors and 0.15 ± 0.06 for zircon rims. Uncertainty for calculated $D_{Th/U}$ is large due to the large spread in Th/U ratios; however, $D_{Th/U}$ is fairly constant for most igneous rock compositions. These $D_{Th/U}$ measurements are similar to an average $D_{Th/U}$ of 0.26 ±

0.16 for zircons from intermediate rocks (55-65 wt% SiO_2) (Bindeman et al., 2006), in spite of their high Th/U ratios that typically suggest a more felsic composition. Because of this, it is safe to assume that the high Th/U ratios in Dayingshan zircons were inherited from a high Th/U melt.

6.4. Comparison of Dayingshan and Maanshan Data: A Common Magma Reservoir

Isotopic and trace element data accumulated from Dayingshan reinforces data from an earlier study of Maanshan by Zou et al. (2010). Maanshan is another active volcano in the Tengchong volcanic field, and lies ~13 km to the south of Dayingshan. The Dayingshan sample has slightly higher SiO_2 and K_2O but lower Na_2O (58.46, 3.40 and 3.79 wt% in Maanshan; 61.50, 4.02 and 3.60 wt% in Dayingshan), and provides evidence for differentiation of the lavas. Zr concentrations are also higher in Dayingshan (329 ppm) than Maanshan (260 ppm). Lavas from both volcanoes also have metaluminous compositions, with Maanshan (1.67) rocks showing a slightly higher $Al_2O_3/(K_2O+Na_2O)$ value than Dayingshan (1.58).

Except for Sr, the Dayingshan sample has slightly higher incompatible elements (e.g, La, Zr, Hf) than Maanshan (Fig. 3), which is consistent with the higher SiO_2 in the Dayingshan sample. This suggests that the Dayingshan sample is slightly more evolved than the Maanshan sample. The slightly higher Sr in the Dayingshan sample is indicative of feldspar fractional crystallization.

Zircon age populations are also highly coherent for both volcanoes. Analysis of zircons from Maanshan recorded a bimodal population for zircon interiors, with calculated ages of 55 ± 7 ka for the younger population and 91 ± 6 ka for the older population. Zircon rims recorded an isochron age of 53.6 ± 5 ka. Dayingshan zircon interior measurements yielded a unimodal age of 87.5 ± 6 ka, while zircon rim measurements yielded an isochron age of 58 ± 13 ka. The older age population (91 ± 6 ka) from Maanshan zircon interiors is consistent with the age (87.5 ± 6 ka) of Dayingshan zircon interiors, and Maanshan zircon rim ages (53.6 ± 5 ka) are consistent with Dayingshan zircon rim ages (58 ± 13 ka).

Because the erupted magmas from Dayingshan and Maanshann volcanoes tap the same zircon populations, we propose that Maanshan and Dayingshan volcanoes share a common magma reservoir. This argues against isolated magma chambers that evolved independently. The seemingly independent magma chambers identified using near-surface geothermal methods (Zhao et al., 2006) may be actually interconnected at depth.

7. CONCLUSIONS

(1) Unpolished zircon rims from Dayingshan yield an isochron age of 58 ± 13 ka while polished zircon interiors yield an age of 87.5 ± 6.5 ka, indicating two age populations at 58 ± 13 ka and 87.5 ± 6.5 ka. The older population most likely represents zircon antecrysts that were formed in an earlier phase of magmatism, but remained in the magma chamber and were remobilized in a

second magmatic phase. The younger population represents phenocrystic growth in the most recent magma body.

(2) Using this age population, a magma chamber storage time of 48±13 ka is deduced by subtracting the most recent eruption age from the zircon age.

(3) The similar zircon age populations between Dayingshan and Maanshan volcanoes indicate that they share a large, common interconnected magma reservoir.

ACKNOWLEDGMENTS

Phil Shane, an anonymous reviewer, and journal editor Andrew Kerr provided constructive reviews that have significantly improved the quality of this paper. Zhengfu Guo generously provided the whole-rock sample for this study. We are also grateful to Clint Barineau for his help with zircon separation, and to Mark Steltenpohl and Bill Hames for their insightful in-house comments. This work was supported by NSF (EAR-0917651) and National Natural Science Foundation of China (41272070). The ion microprobe laboratory at UCLA is in part supported by a grant from NSF Instrumentation and Facility program.

References

Bacon, C.R., Sisson, T.W., Mazdab, F.K., 2007. Young cumulate complex beneath Veniaminof caldera, Aleutian arc, dated by zircon in erupted plutonic blocks. Geology 35, 491-494.

Bai, D., Meju, M.A., Liao, Z., 2001. Magnetotelluric images of deep crustal structure of the Rehai geothermal field near Tengchong, southern China. Geophysical Journal International 147, 677-687.

Bindeman, I.N., Schmitt, A.K., Valley, J.W., 2006. U-Pb zircon geochronology of silicic tuffs from the Timber Mountain/Oasis Valley caldera complex, Nevada: rapid generation of large volume magmas by shallow-level remelting. Contributions to Mineralogy and Petrology 152, 649-665.

Charlier, B.L.A., Wilson, C.J.N., Lowenstern, J.B., Blake, S., Van Calsteren, P.W., Davidson, J.P., 2005. Magma generation at a large, hyperactive silicic volcano (Taupo, New Zealand) revealed by U-Th and U-Pb systemtics in zircons. Journal of Petrology 46, 3-32.

Chen, F., Satir, M., Ji, J., Zhong, D., 2002. Nd–Sr–Pb isotopes of Tengchong Cenozoic volcanic rocks from western Yunnan, China: evidence for an enriched-mantle source. Journal of Asian Earth Sciences 21, 39-45.

Fan, Q.C., Liu, R.X., Wei, H.Q., Shi, L.B., Sui, J.L., 1999. The magmatic evolution of the active volcano in the Tengchong area. Geological Review 45, 895-904.

Fan, Q.C., Sui, J.L., Liu, R.X., 2001. Sr-Nd isotopic geochemistry and magmatic evolutions of Wudalianchi volcano, Tianchi volcano and Tengchong volcano. Acta Petrologica et Mineralogica 20, 233-238.

Grove, M., Harrison, T.M., 1999. Monazite Th-Pb age depth profiling. Geology 27, 487-490.

Guo, Z.F., Zhang, M.L., Cheng, Z.H., Liu, J.Q., Zhang, L.H., Li, X.H., 2011. A link of measurements of lava flows to Palaeoelevation estimates and its application in Tengchong volcanic eruptive field in Yunnan Province (SW China). Acta Petrologica Sinica 27, 2863-2872.

Huangpu, G., Jiang, C.S., 2000. Study of Tengchong volcanic activities. Yunan Science and Technology Press, Kunming, 418 pp.

Jiang, C., 1998. Stages of eruptions of the Tengchong volcanoes. Journal of Seismological Research 21, 309-319.

Lei, J.S., Zhao, D.P., Su, Y.J., 2009. Insight into the origin of the Tengchong intraplate volcano and seismotectonics in southwest China from local and teleseismic data. Journal of Geophysical Research 114, B05302.

Li, D.M., Li, Q., Chen, W.J., 2000. Volcanic activity of Tengchong since the Pliocene. Acta Petrologica Sinica 16, 362-370.

Li, D.P., Luo, Z.H., Liu, J.Q., Chen, Y.L., Jin, Y., 2012. Magma origin and evolution of Tengchong Cenozoic volcanic rocks from west Yunnan, China: Evidence from whole rock geochemistry and Nd-Sr-Pb isotopes. Acta Geologica Sinica 86, 867-878.

Li, X., Liu, J.Q., 2012. A study on the geochemical characteristics and petrogenesis of Holocene volcanic rocks in the Tengchong volcanic eruption field, Yunnan Province, SW China. Acta Petrologica Sinica 28, 1507-1516.

Ludwig, K.R., 2003. User's Manual for ISOPLOT 3.00: A geochronological toolkit for Microsoft Excel. Berkeley Geochronology Center Special Publication No. 4, Berkeley, 70 pp.

Mu, Z.G., Curtis, G.H., Liao, Z.J., Tong, W., 1987a. K-Ar age and strontium isotopic composition of the Tengchong volcanic rocks, West Yunnan Province, China. Geothermics 16, 283-297.

Mu, Z.G., Tong, W., Curtis, G.H., 1987b. Times of volcanic activity and origin of magma in Tengchong geothermal area, west Yunnan province. Acta Geophysica Sinica 30, 261-270.

Reid, M.R., Coath, C.D., 2000. In situ U-Pb ages of zircons from the Bishop Tuff: No evidence for long crystal residence times. Geology 28, 443-446.

Reid, M.R., Coath, C.D., Harrison, T.M., McKeegan, K.D., 1997. Prolonged residence times for the youngest rhyolites associated with Long Valley caldera: Ion microprobe dating of young zircons. Earth and Planetary Science Letters 150, 27-38.

Schmitt, A.K., 2009. Quaternary geochronology by SIMS. In: Fayek, M. (Ed.), Mineralogical Association of Canada Short Course 41, Toronto, pp. 109-131.

Schmitt, A.K., 2011. Uranium series accessory crystal dating of magmatic processes. Annual Review of Earth and Planetary Sciences 39, 321-349.

Schmitt, A.K., Grove, M., Harrison, T.M., Lovera, O.M., Hulen, J., Waters, M., 2003. The Guysers-Cobb Mountain Magma System, California (part 1): U-Pb zircon ages of volcanic rocks, conditions of zircon crystallization and magma residence times. Geochimica et Cosmochimica Acta 67, 3423-3442.

Shane, P., Storm, S., Schmitt, A.K., Lindsay, J.M., 2012. Timing and conditions of formation of granitoid clasts erupted in recent pyroclastic deposits from Tarawera Volcano (New Zealand). Lithos 140-141, 1-10.

Shangguan, Z., Zhao, C., Li, H., Gao, Q., Sun, M., 2005. Evolution of hydrothermal explosions at Rehai geothermal field, Tengchong volcanic region, China. Geothermics 34, 518-526.

Simon, J.I., Renne, P.R., Mundil, R., 2008. Implications of pre-eruptive magmatric histories of zircons for U-Pb geochronology of silicic extrusions. Earth and Planetary Science Letters 266, 182-194.

Storm, S., Shane, P., Schmitt, A.K., Lindsay, J.M., 2011. Contrasting punctuated zircon growth in two syn-erupted rhyolite magmas from Tarawera volcano: Insight to crystal diversity in magmatic systems. Earth and Planetary Science Letters 301, 511-520.

Tapponnier, P., Lacassin, R., Leloup, P.H., Scharer, U., Zhong, D.L., Wu, H.W., Liu, X.H., Ji, S.C., Zhang, L.S., Zhong, J.Y., 1990. The Ailao Shan/Red River metamorphic belt: Tertiary left-lateral shear between Indochina and South China. Nature 343, 431-437.

Vazquez, J.A., Reid, M.R., 2002. Time scales of magma storage and differentiation of voluminous high-silica rhyolites at Yellowstone caldera, Wyoming. Contributions to Mineralogy and Petrology 144, 274-285.

Wang, F., Peng, Z.C., Zhu, R.X., He, H.Y., Yang, L.K., 2006. Petrogenesis and magma residence time of lavas from Tengchong volcanic field (China): Evidence from

U series disequilibria and $^{40}Ar/^{39}Ar$ dating. Geochemistry Geophysics Geosystems 7, Q01002, doi: 10.1029.

Wang, Y., Zhang, X.M., Jiang, C.S., Wei, H.Q., Wan, J.L., 2007. Tectonic controls on the late Miocene–Holocene volcanic eruptions of the Tengchong volcanic Weld along the southeastern margin of the Tibetan plateau. Journal of Asian Earth Sciences 30, 375–389.

Watson, E.B., Harrison, T.M., 1983. Zircon saturation revisited: temperature and composition effects in a variety of crustal magma types. Earth and Planetary Science Letters 64, 295-304.

Wei, H., Sparks, R.S.J., Liu, R., Fan, Q., Wang, Y., Hong, H., Zhang, H., Chen, H., C., J., Dong, J., Zheng, Y., Pan, Y., 2003. Three acive volcanoes in China and their hazards. Journal of Asian Earth Sciences 21, 515-526.

Xu, Y., Yang, X.T., Li, Z.W., Liu, J.H., 2012. Seismic structure of the Tengchong volcanic area southwest China from local earthquake tomography. Journal of Volcanology and Geothermal Research 239-240, 83-91.

Zhao, C.P., Ran, H., Chen, K.H., 2006. Present-day magma chambers in Tengchong volcano area inferred from relative geothermal gradient. Acta Petrologica Sinica 22, 1517-1528.

Zhao, Y.W., Fan, Q.C., 2010. Magma origin and evolution of Maanshan volcano, Dayingshan volcano and Heikongshan volcano in Tengchong area. Acta Petrologica Sinica 26, 1133-1140.

Zhou, M.F., Robinson, P.T., Wang, C.Y., Zhao, J.H., Yan, D.P., Gao, J.F., Malpas, J., 2012. Heterogeneous mantle source and magma differentiation of quaternary arc-like volcanic rocks from Tengchong, SE margin of the Tibetan Plateau. Contributions to Mineralogy and Petrology 163, 841-860.

Zhu, B.Q., Mao, C.X., Lugmair, G.W., Macdougall, J.D., 1983. Isotopic and geochemical evidence for the origin of plio-pleistocene volcanic-rocks near the Indo-Eurasian collisional margin at Tengchong, China. Earth and Planetary Science Letters 65, 263-275.

Zou, H.B., Fan, Q.C., 2011. Uranium-thorium isotope disequilibrium in young volcanic rocks from China. Acta Petrologica Sinica 27, 2821-2826.

Zou, H.B., Fan, Q.C., Schmitt, A.K., Sui, J.L., 2010a. U-Th dating of zircons from Holocene potassic andesites (Maanshan volcano, Tengchong, SE Tibetan Plateau) by depth profiling: Time scales and nature of magma storage. Lithos 118, 202-210.

Zou, H.B., Fan, Q.C., Zhang, H.F., 2010b. Rapid development of the great Millennium eruption of Changbaishan (Tianchi) Volcano: Evidence from U-Th zircon dating. Lithos 119, 289-296.

Figure Captions

Fig. 1. (a) Regional map showing major tectonic features in Asia (Tapponnier et al., 1990). (b) Location map of the Tengchong volcanic field in SE China. TVF lies in a N-S trending fault zone between the Sagaing and Red River faults, and lies ~200 km from the subduction-related Burma volcanic arc. (c) Distribution and relative ages of the three most recently active volcanoes and surrounding rocks. Most volcanoes represented are small cinder cones. (d) Distribution of depositional units deposited by four eruptive events from Dayingshan volcano. I is the oldest flow, and IV is the youngest (Huangpu and Jiang, 2000).

Fig. 2. Spider diagram of Dayingshan (DA09026) and Maanshan (MA02) (Zou et al., 2010) trace elements. The vertical axis is normalized using estimated primitive mantle.

Fig. 3. U/Th isochron plot for zircon rims from Dayingshan using shallow depth profiling. Chart was constructed and ages were determined using Isoplot (Ludwig, 2003).

Fig. 4. Cathodoluminescence images of sample Day-int4 and Day-int7 and Day-int10 with SIMS crater spots.

Fig. 5. U/Th isochron plot for zircon interiors from Dayingshan. Chart was constructed and ages were determined using Isoplot (Ludwig, 2003)

Fig. 6. (A) Zircon interior age distribution from Dayingshan produced using the probability density function from Isoplot (Ludwig, 2003). Zircon rim isochron age with uncertainty is also shown. (B) Zircon interior model age distributions from Maanshan (Zou et al., 2010a) for comparison.

Fig. 7. Histograms for pre-eruption ages for small volume volcanic eruptions. The apparent pre-eruption age for Dayingshan is shown with an arrow.

LIST OF TABLES

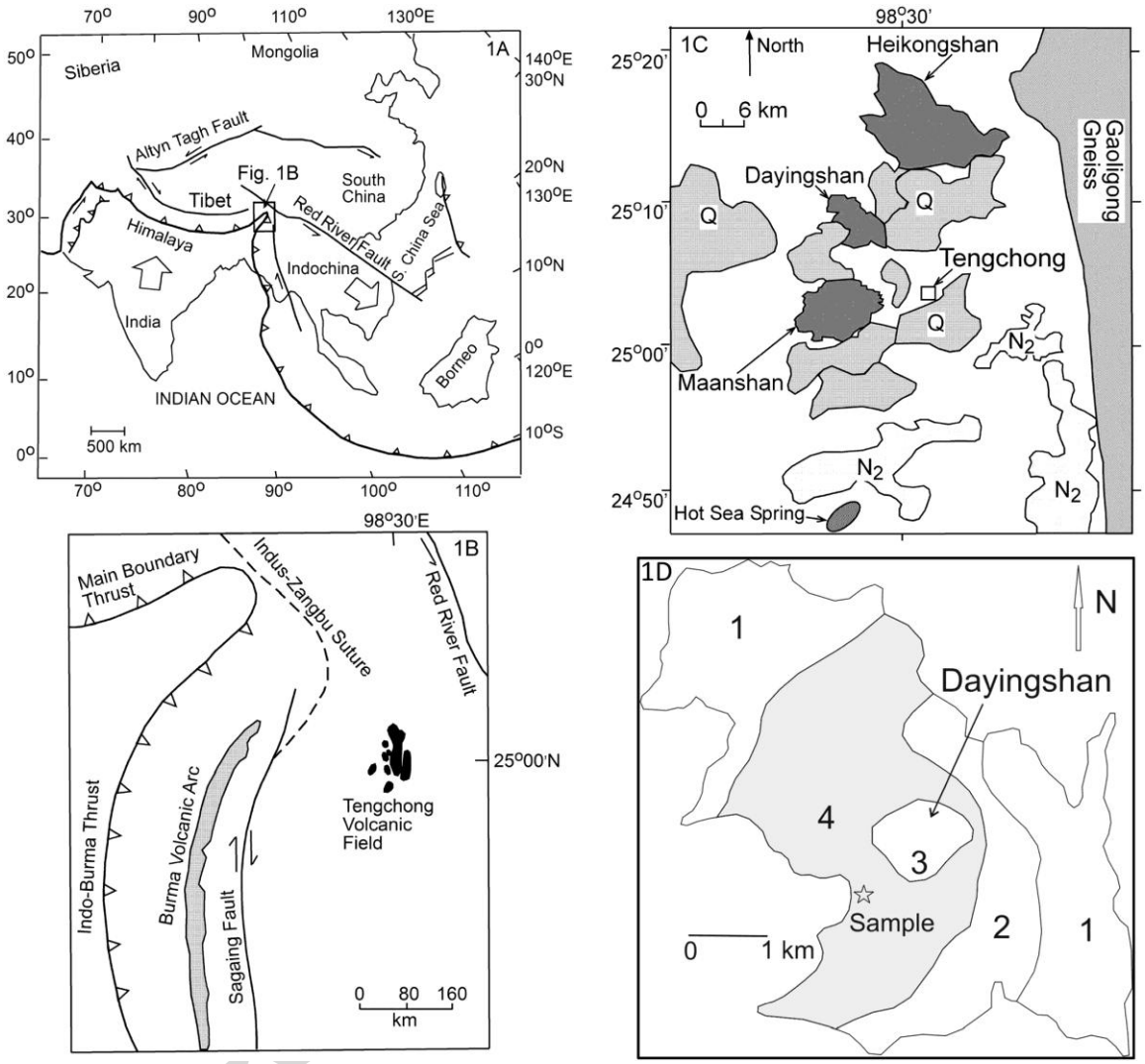

Figure 1

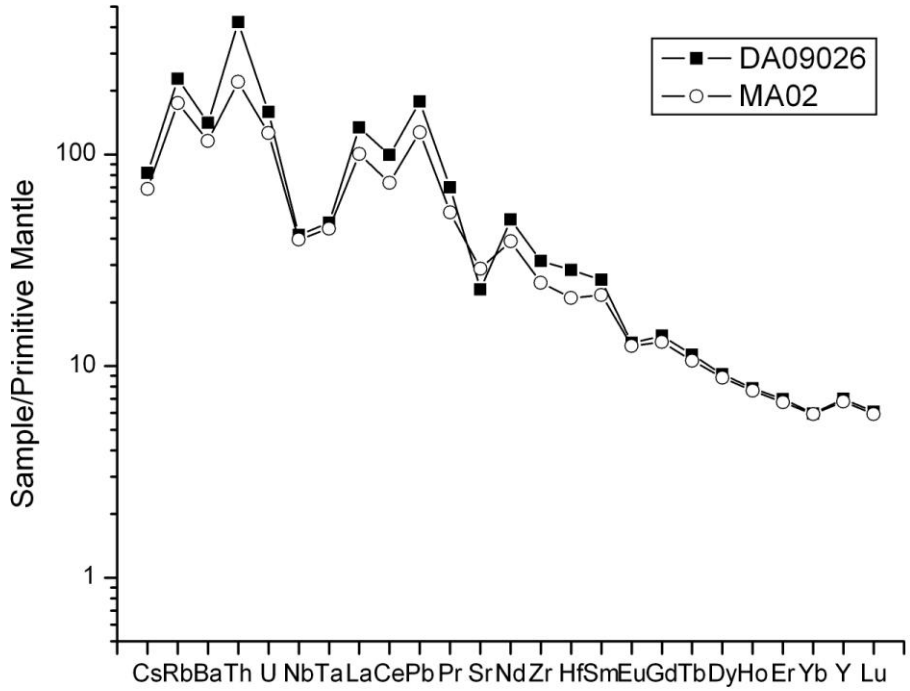

Figure 2

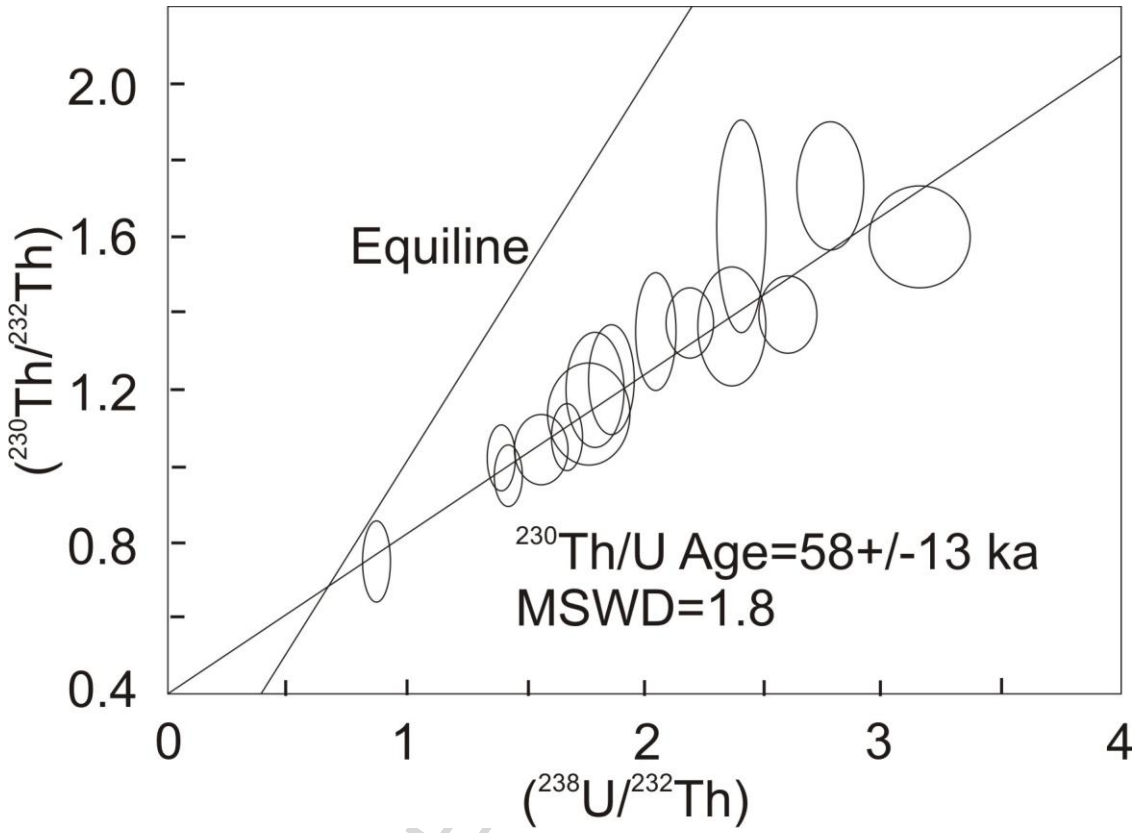

Figure 3

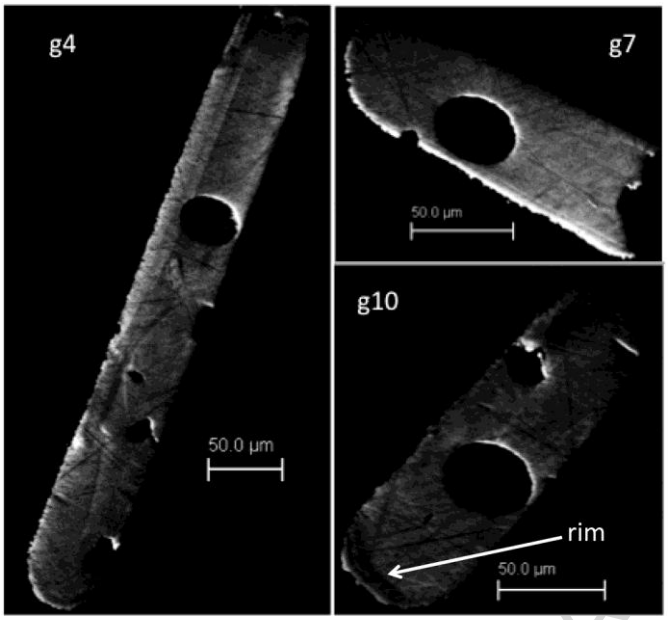

Figure 4

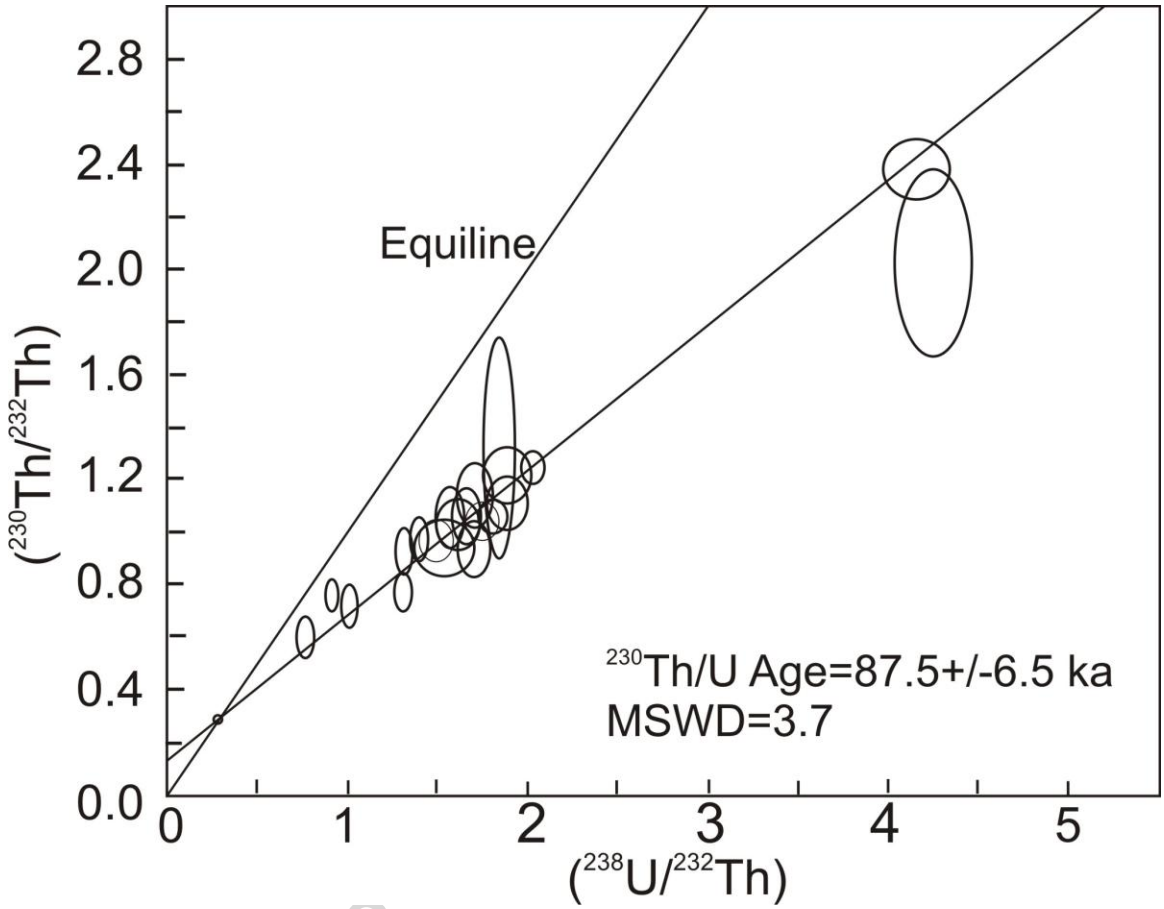

Figure 5

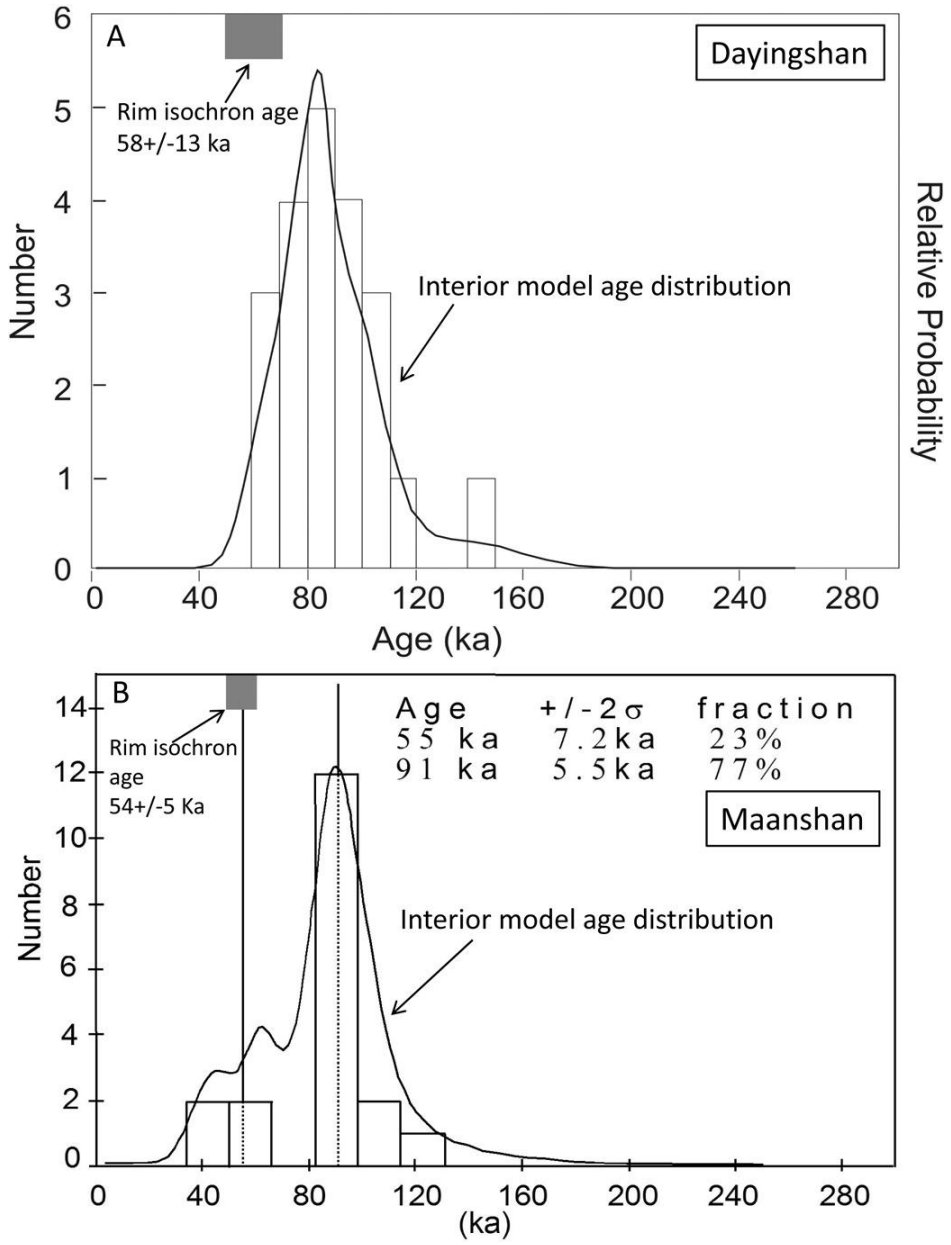

Figure 6

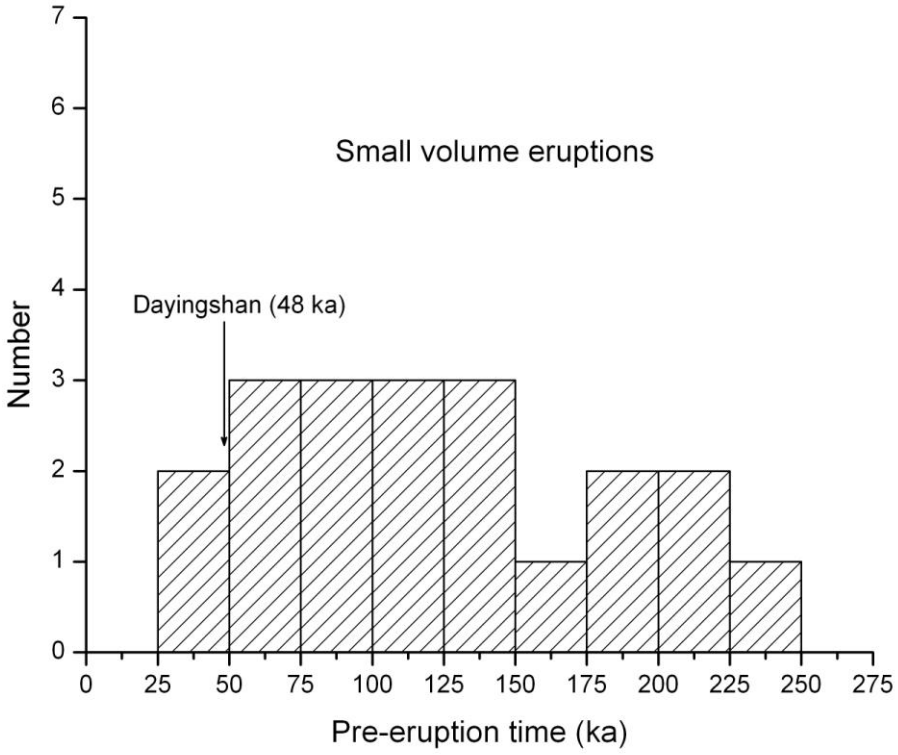

Figure 7

Table 1

Major and trace element concentrations from Dayingshan whole-rock analysis of sample.

	wt%		ppm		ppm		ppm
SiO2	61.50	La	86.8	Tm	0.44	Rb	137
TiO2	1.01	Ce	166.3	Yb	2.63	Cs	1.72
Al2O3	16.27	Pr	17.8	Lu	0.41	Sr	457
FeO*	5.22	Nd	61.5	Ba	933	Sc	13.5
MnO	0.092	Sm	10.4	Th	33.5	Zr	329
MgO	2.43	Eu	1.98	Nb	28.5	Zr (XRF)	322
CaO	4.54	Gd	7.57	Y	30.1	Ni (XRF)	25
Na2O	3.60	Tb	1.12	Hf	8.06	Cr (XRF)	21
K2O	4.02	Dy	6.16	Ta	1.76	Sc (XRF)	12
P2O5	0.40	Ho	1.17	U	3.22	V (XRF)	91
Sum	99.09	Er	3.06	Pb	26.7		

Table 2

U/Th isotope data, concentrations and ages for Dayingshan zircon rims as measured by SIMS. 1s is the standard error and is a measurement of uncertainty.

Sample	($^{238}U/^{232}Th$)	1s	($^{230}Th/^{232}Th$)	1s	($^{238}U/^{232}Th$)	1s	U ppm	Th ppm	Th/U	D Th/U
Day-rim1	1.420	0.020	3.360	0.210	4.452	0.063	988	674	0.68	0.06
Day-rim2	0.502	0.015	1.045	0.036	1.573	0.046	924	1781	1.93	0.18
Day-rim3	0.595	0.012	1.225	0.058	1.865	0.037	371	604	1.63	0.15
Day-rim4	0.768	0.013	1.617	0.117	2.409	0.041	415	522	1.26	0.12
Day-rim5	1.008	0.028	1.593	0.054	3.161	0.087	732	703	0.96	0.09
Day-rim6	0.538	0.008	1.075	0.035	1.686	0.025	622	1119	1.80	0.17
Day-rim7	0.280	0.007	0.759	0.053	0.877	0.022	266	921	3.46	0.33
Day-rim8	0.566	0.024	1.135	0.054	1.774	0.074	450	770	1.71	0.16
Day-rim9	0.449	0.008	1.017	0.033	1.408	0.024	660	1422	2.15	0.20
Day-rim10	0.757	0.020	1.364	0.064	2.373	0.064	545	697	1.28	0.12
Day-rim11	0.887	0.018	1.731	0.070	2.782	0.056	541	590	1.09	0.10
Day-rim12	0.699	0.010	1.374	0.038	2.191	0.033	981	1358	1.38	0.13
Day-rim13	0.829	0.015	1.392	0.044	2.600	0.047	1050	1226	1.17	0.11
Day-rim14	0.656	0.010	1.349	0.062	2.056	0.033	591	873	1.48	0.14
Day-rim15	0.573	0.017	1.192	0.062	1.797	0.053	484	817	1.69	0.16
Day-rim16	0.851	0.016	1.837	0.095	2.669	0.049	328	373	1.14	0.11
Day-rim17	0.458	0.008	0.975	0.033	1.435	0.025	908	1921	2.11	0.20
Average									1.58	0.15
Std deviation									0.63	0.06

The zircon surface rims themselves yield a good isochron with MSWD of 1.8, and thus two-point zircon-whole-rock model ages are not used here.

Table 3

U/Th isotope data, concentrations, and ages for Dayingshan zircon cores as measured by SIMS. 1s is the standard error and is a measurement of uncertainty.

Sample	($^{238}U/^{232}Th$)	1s	($^{230}Th/^{232}Th$)	1s	($^{238}U/^{232}Th$)	1s	U ppm	Th ppm	Th/U	D Th/U	Age (ka)	+ (ka)	- (ka)
Zircons													
Day-int1	1.326	0.025	2.384	0.046	4.158	0.077	2644	1929	0.73	0.07	84.3	3.8	-3.7
Day-int2	0.597	0.017	1.214	0.045	1.873	0.053	529	858	1.62	0.15	93.5	9.3	-8.6
Day-int3	0.543	0.011	0.930	0.044	1.702	0.036	395	704	1.78	0.17	64.1	6.7	-6.3
Day-int4	0.501	0.012	1.054	0.046	1.570	0.037	430	831	1.93	0.18	96.5	11.0	-10.0
Day-int5	0.491	0.023	0.943	0.046	1.539	0.071	369	727	1.97	0.19	78.3	11.1	-10.1
Day-int6	0.446	0.008	0.979	0.032	1.397	0.026	681	1479	2.17	0.21	102.9	9.5	-8.7
Day-int7	0.245	0.005	0.599	0.030	0.768	0.015	353	1396	3.95	0.37	105.0	20.5	-17.2
Day-int8	0.324	0.006	0.720	0.034	1.014	0.019	397	1186	2.99	0.28	93.6	13.4	-11.9
Day-int9	0.293	0.005	0.761	0.024	0.918	0.017	769	2543	3.31	0.31	142.2	18.8	-16.0
Day-int10	0.542	0.013	1.131	0.054	1.699	0.041	499	891	1.79	0.17	96.7	11.7	-10.6
Day-int11	0.557	0.012	1.039	0.032	1.747	0.037	753	1309	1.74	0.16	76.7	5.7	-5.4
Day-int12	0.650	0.008	1.242	0.026	2.038	0.027	1377	2051	1.49	0.14	84.1	4.1	-4.0
Day-int13	0.604	0.014	1.107	0.041	1.895	0.045	509	815	1.60	0.15	75.9	6.6	-6.3
Day-int14	0.583	0.011	1.314	0.174	1.829	0.035	496	823	1.66	0.16	116.6	44.0	-31.3
Day-int15	0.530	0.010	1.054	0.045	1.660	0.031	395	721	1.83	0.17	86.7	8.8	-8.2
Day-int16	1.360	0.036	3.736	0.174	4.264	0.112	231	165	0.71	0.07	217.7	50.1	-34.2
Day-int17	0.479	0.011	0.966	0.034	1.501	0.033	510	1030	2.02	0.19	86.6	7.9	-7.4
Day-int18	1.354	0.029	2.025	0.142	4.244	0.090	266	190	0.72	0.07	62.4	7.5	-7.0

Day-int19	0.420	0.006	0.924	0.034	1.318	0.019	507	1168	2.30	0.22	101.0	10.0	-9.2
Day-int20	0.575	0.009	1.064	0.026	1.803	0.027	1233	2074	1.68	0.16	76.2	4.3	-4.1
Day-int21	0.512	0.014	1.030	0.040	1.604	0.044	700	1325	1.89	0.18	88.0	9.1	-8.4
Day-int22	0.418	0.006	0.772	0.033	1.309	0.019	405	939	2.32	0.22	67.3	7.0	-6.6
Average									1.92	0.18			
Std deviation									0.77	0.07			

[a] Model ages are calculated from two-point zircon-whole rock isochron; uncertainties are 1σ.

Highlights

- We date very young zircons from rare active volcanoes on SE Tibetan Plateau.
- Magma residence time for Dayingshan volcano is about 48 thousand years.
- We use zircon ages to investigate the plumbing system of an active volcanic field.
- Zircon ages from Dayingshan volcano is similar to those from Maanshan volcano.
- Dayingshan and Maanshan volcanoes share a common interconnected magma reservoir.